The EMBO Journal vol.12 no.9 pp.3679-3684, 1993

Apoptotic death in epithelial cells: cleavage of DNA to 300 and/or 50 kb fragments prior to or in the absence of internucleosomal fragmentation

Franziska Oberhammer[1], James W.Wilson[2], Caroline Dive[2], Ian D.Morris[2], John A.Hickman[2,5], Alan E.Wakeling[3], P.Roy Walker[4] and Marianna Sikorska[4]

[1]Institute for Tumour Biology, University of Vienna, Berschkegasse 8a, Vienna, Austria 1090A, [2]Molecular Pharmacology and Toxicology Group, School of Biological Sciences, University of Manchester, Manchester M13 9PT, UK, [3]Zeneca Pharmaceuticals, Alderley Park, Macclesfield, Cheshire, SK10 4TG, UK and [4]Molecular Cell Biology Group, Institute for Biological Sciences, National Research Council of Canada, Ottawa, Canada K1A 0R6

[5]Corresponding author

Communicated by U.Laemmli

To date, apoptosis has been characterized biochemically by the production of 180-200 bp internucleosomal DNA fragments resulting from the activation of an endonuclease(s). The principal morphological feature of apoptosis is the condensation of chromatin and it has been assumed that this may reflect the oligonucleosomal fragmentation pattern. We have re-examined this dogma by comparing the biochemical and morphological features of cell death in several epithelial cell types (HT-29-I1 colon adenocarcinoma, CC164 mink lung, DU-145 human prostatic carcinoma and MCF-7 human breast adenocarcinoma) and one mesenchymal cell line (H11ras-R3 *ras*-transformed rat fibroblasts). Cell death was induced either by serum deprivation, TGF-β1 or etoposide, or by leaving cells to reach confluence. Cell death was assessed with respect to detachment from monolayers, morphological changes and DNA integrity. The DNA-binding fluorophore Hoechst 33258 revealed chromatin condensation patterns consistent with apoptotic cell death in all cell types except MCF-7 cells. Using field inversion gel electrophoresis in conjunction wih conventional 2% agarose gel electrophoresis, cleavage of DNA to 50 kbp fragments was observed in all cases except MCF-7 cells. This preceded the appearance of oligonucleosomal fragments in HT-29-I1, CC164 and H11ras-R3 cells. Although the DNA of DU-145 cells fragmented into 50 kbp units, and although the cells exhibited classical apoptotic morphology, no subsequent internucleosomal cleavage was observed. These results suggest that changes in the integrity of DNA indicative of the release of chromatin loop domains occur before cleavage at internucleosomal sites is initiated and that the latter is not an essential step in the apoptotic process.

Key words: apoptosis/chromatin condensation/DNA fragmentation/endonucleolytic cleavage

Introduction

A cardinal morphological feature of apoptotic cell death is the condensation of chromatin and its margination at the nuclear periphery (reviewed by Wyllie, 1992). The biochemical hallmark of apoptosis is the appearance of a fragmentation pattern in chromatin indicative of the DNA cleavage at the linker regions between nucleosomes. This produces a characteristic pattern of DNA cleavage into 180 bp oligonucleosome, integer fragments (a DNA 'ladder') when DNA from apoptotic cells is subjected to conventional gel electrophoresis (Wyllie, 1980). This internucleosomal cleavage of DNA is considered to arise from the activation of an endonuclease or endonucleases (reviewed by Compton, 1992). Recently, it has been variously suggested that the endonuclease initiating apoptosis may be NUC-18 (Caron-Leslie *et al.*, 1991), DNase I (Ucker *et al.*, 1992; Peitsch *et al.*, 1993) or DNase II (Barry and Eastman, 1993). The relationship between the appearance of condensed chromatin and the endonucleolytic cleavage of DNA is uncertain. Arends *et al.* (1990) have implied that chromatin condensation observed in thymocytes is the result of the internucleosomal endonucleolytic cleavage of DNA, but a number of recent studies in other cell types do not support this as a universal hypothesis. For example, chromatin condensation during cell death was observed in oligodendrocytes (Barres *et al.*, 1992) and in hepatocytes (Oberhammer *et al.*, 1993) but, despite intensive investigation, no evidence of the classical endonucleolytic cleavage pattern of DNA was found. Flow cytometric analysis of apoptotic thymocytes has suggested that some changes in chromatin structure precede the initiation of internucleosomal DNA cleavage (Cohen *et al.*, 1992) and studies by Tomei *et al.* in murine embryonic fibroblast cells have also cast doubt on whether double stranded internucleosomal cleavage of DNA to 180 bp integer fragments is an essential step in their apoptosis (Tomei *et al.*, 1993).

Changes in the integrity of DNA are optimally evaluated using field inversion gel electrophoresis (FIGE). This technique allows analysis of the integrity of DNA of molecular weights of up to ~2 Mbp (Carle *et al.*, 1986) whereas conventional gel electrophoresis of DNA (which is used to establish the 'laddering' pattern of cleavage in apoptosis) is restricted to the analysis of DNA fragments of ~20 kbp and below. When the DNA from thymocytes or lymphocytes treated with topoisomerase II inhibitors or dexamethasone was analyzed by FIGE, distinctive fragments of 50 and 300 kbp were generated (Walker *et al.*, 1991; Roy *et al.*, 1992). The 300 kbp fragments were considered to be generated by the interaction of the drugs with topoisomerase II molecules located at specific sites in chromatin (Filipski *et al.*, 1990) whereas the 50 kbp fragments and the accompanying DNA 'ladder' were generated by endonucleolytic activity during apoptosis. However, in studies that use DNA-damaging drugs to induce apoptosis it is difficult to separate breaks introduced by treatment from those that represent the initial breaks of apoptosis. To obviate this problem, we have analyzed, temporally, the integrity of DNA from several epithelial cell types which were induced

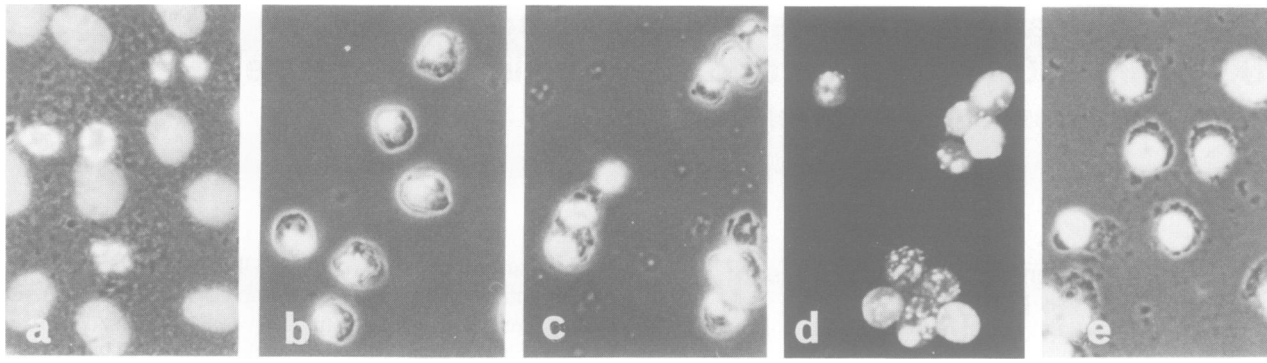

Fig. 1. Morphological features of nuclear chromatin in various cells undergoing cell death stained with the DNA-binding fluorochrome Hoechst 33258. (**a**) H11ras-R3 rat fibroblasts attached to substratum 4 h after removal of serum (see also Figure 3); (**b**) detached CC164 mink lung cells collected 2 h after the addition of TGF-β1; (**c**) detached HT-29-I1 human colon adenocarcinoma cells collected at confluence; (**d**) detached DU-145 androgen-independent human prostatic carcinoma cells treated with 25 μM VP16 and collected between 18 and 36 h after drug treatment; (**e**) MCF-7 human mammary carcinoma cells, collected after 2 h of serum withdrawal. (Magnification ×600).

to die and detach from monolayer cultures by a variety of conditions. Despite the appearance of condensed chromatin in each cell type, not all cell types underwent internucleosomal cleavage to generate a DNA 'ladder'. However, in all cell types investigated which demonstrated chromatin condensation typical of apoptosis, FIGE revealed the appearance of large DNA fragments (300 and/or 50 kbp). In those cells which fragmented their DNA to 180 integers, to produce a 'ladder', the appearance of the larger fragments was always a prior event. This observation is discussed with respect to the possible nature of events which initiate apoptosis.

Results

Several cell types were subjected to disparate conditions and the resultant mode of cell death was investigated with respect to the detachment of monolayer cells, changes in morphology and the integrity of their DNA. VP-16 treatment of DU-145 human, androgen-independent prostatic carcinoma cells, serum starvation of MCF-7 breast carcinoma cells or H11ras-R3 rat fibroblasts, prolonged confluency in HT-29-I1 human colon adenocarcinoma cells and TGF-β1 treatment of CC164 mink lung cells, all resulted in the detachment of cells from the epithelial monolayers. All cell types except MCF-7 cells exhibited condensation of chromatin, either just immediately prior to or after detachment from the monolayer. These morphological changes are shown in Figure 1. Figure 1a shows that 4 h after serum withdrawal from H11ras-R3 fibroblasts, apoptotic cells with chromatin condensed at the nuclear periphery were observed in confluent monolayers immediately prior to their rounding up and detachment.

Detached CC164 mink lung epithelial cells maintained cellular membrane integrity and exhibited condensed chromatin (Figure 1B). In the case of the HT-29-I1 colon adenocarcinoma cells (Figure 1C), >90% of detached cells exhibited nuclear morphologies indicative of apoptosis as determined using the DNA-binding fluorophore Hoechst 33258. Similar chromatin condensation and nuclear fragmentation were also seen in the detached DU-145 prostate cells (Figure 1D). MCF-7 cell death, however, was morphologically different from that of the other cell types: the detached cells had an altered chromatin structure but the nuclei appeared pyknotic with a crenulated periphery (Figure 1e). Nucleoli were visible in MCF-7 cells, whereas they were lost in the colon, prostate, lung and mesenchymal cells (Figure 1a–d).

Cells that had detached from epithelial monolayers were collected at short intervals before DNA was extracted. Figure 2 shows an analysis of DNA integrity of HT-29-I1 and CC164 cells by FIGE, together with conventional gel electrophoresis using either total extracted DNA or that which eluted from agarose plugs incubated with sarcosyl and proteinase K prior to FIGE (see Materials and methods). In every analysis of DNA integrity by FIGE, all cell samples, including untreated controls, exhibited a discrete band from 700 to 1000 kbp. This has been attributed to the migration of any DNA fragment of >750 kbp entering the gel (Walker *et al.*, 1991). In the cases of both HT-29-I1 cells at confluence and TGF-β1 treated CC164 cells, FIGE revealed accumulating cleavage to 50 kbp fragments. No prior or simultaneous 300 kbp fragments were detected. At the first appearance of the 50 kbp fragments in HT-29-I1 cells there was no indication of simultaneous internucleosomal fragmentation, measured by conventional electrophoresis. With time, however, the distinct 50 kbp fragment became more diffuse, indicative of subsequent degradation to lower molecular weight fragments. Conventional DNA gel electrophoresis then showed that this corresponded to the appearance of internucleosomal cleavage, to give the typical apoptotic 'ladders' in these cell types (Figure 2A and C). Ultimately, the discrete patterns of fragmentation, observed by both FIGE and conventional gel electrophoresis, were lost as digestion of DNA proceeded.

A more detailed investigation of the temporal nature of DNA fragmentation in H11ras-R3*ras*-transformed rat fibroblasts, where both attached and detached cells were collected, to equal cell number, every 30 min, showed that the appearance of 300 kbp fragments was observed rapidly after removal of serum (Figure 3). The kinetics of cell detachment following serum withdrawal are shown in Figure 3B, confirming the relatively synchronous pattern of cell death induced in this model. The 300 kbp fragments appeared to be transient, disappearing after 2 h. Coincident with the emergence of the 300 kbp bands, persistent 50 kbp fragments were also observed. As with the HT29-I1 and CC164 cells, no coincident internucleosomal fragmentation pattern occurred until the 50 kbp fragments degraded further, when

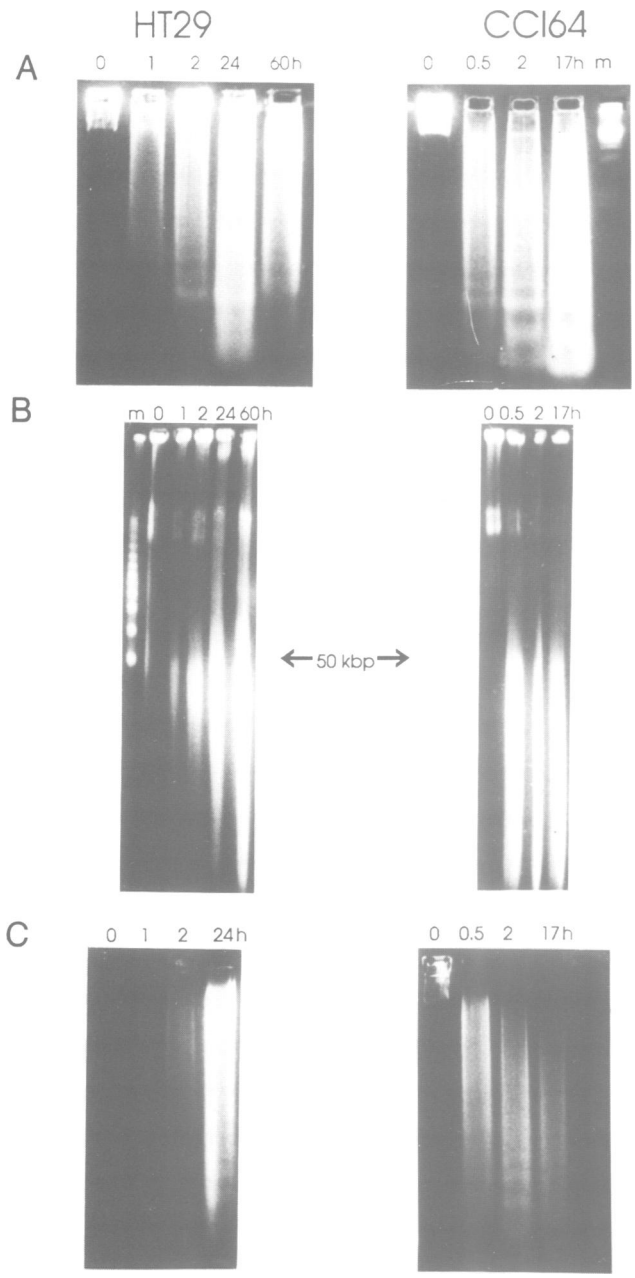

Fig. 2. FIGE and simultaneous conventional gel electrophoresis of DNA from detached HT-29-I1 and CC164 cells at the times shown either after reaching confluence (HT-29) or after the addition of TGF-β1 (CC164). The upper panels (**A**) show conventional electrophoresis of the DNA and the lower panel (**C**) shows conventional electrophoresis of the DNA recovered from the supernatants of the agarose plugs prepared for FIGE (**B**) (see Materials and methods). (m, molecular weight markers.)

the appearance of DNA 'laddering' was seen using conventional techniques of DNA electrophoresis.

DU-145 prostatic carcinoma cells treated with 25 μM VP-16 asynchronously detached from the monolayer over 36 h and exhibited a similar morphology to the detached HT-29-I1 and CC164 cells (Figure 1d). DNA extracted from detached DU-145 cells analyzed by FIGE revealed discrete 50 kbp fragments and with no obvious smearing to lower molecular weight fragments (Figure 4). No 300 kbp fragments were observed during this asynchronous induction of apoptosis. When conventional electrophoresis was applied, DU-145 cells did not manifest a pattern of 180 bp integer internucleosomal fragmentation. Serum deprivation of MCF-7 human mammary carcinoma cells did not result in a distinct fragmentation pattern to discrete 50 kbp (data not shown) and, like the DU-145 cells, the mammary carcinoma cells failed to show internucleosomal DNA 'laddering' at any time.

Discussion

Observations that many types of cell undergo apoptotic cell death, an active process, have received renewed attention (Wyllie, 1992). An understanding that tumor cell population dynamics depends upon changes in the balance of cell loss and gain has raised the possibility of pharmacological intervention to increase cell loss by apoptosis. Many anticancer drugs initiate apoptosis (reviewed by Dive and Wyllie, 1993; Hickman, 1992) and it is possible that the failure of certain cancer cells to engage in apoptosis may explain the inherent drug resistance of many tumors. Consequently, it is important to gain insight into the biochemical processes which initiate apoptotic cell death. Emphasis has been placed on the identification of an endonuclease thought to be responsible for the condensation of chromatin in apoptotic cells (reviewed by Compton, 1992). This has been considered to be the cardinal feature of this type of cell death, where studies have focused heavily on hemopoietic cells. The nature of the signals which engage the activation of such endonuclease(s) remains unclear, but it has been generally assumed that a programmed cell death depends upon the activation of endonucleolytic, internucleosomal cleavage of DNA.

In this study of a number of epithelial cell lines and one of mesenchymal origin, we were stimulated to investigate the nature of changes in DNA integrity because, although we were able to observe morphological features of apoptosis readily (Figure 1), we were not always able to confirm this as classical apoptosis by demonstrating simultaneous internucleosomal cleavage of DNA to 180 bp integers. This concurs with the observations of other investigators (Cohen *et al.*, 1992; Brown *et al.*, 1993; Gavrieli *et al.*, 1992). For example in DU-145 prostatic carcinoma cells, which displayed the morphology of apoptosis (Figure 1D), we were unable to detect DNA laddering at any time point, again similar to the observation of others (Barres *et al.*, 1992; Oberhammer *et al.*, 1993; Tomei *et al.*, 1993). Such observations are inconsistent with the dogma that internucleosomal fragmentation to 180–200 bp integers necessarily reflects the chromatin condensation patterns seen in apoptotic cells.

Here we show that an analysis of DNA integrity by FIGE in epithelial cells, induced to die either by the addition of TGF-β1 or as they reached confluence and spontaneously detached from monolayers, revealed a distinctive pattern of DNA cleavage prior to internucleosomal fragmentation. Specifically, 50 kbp fragments were observed in the cell types which exhibited an apoptotic morphology. When a detailed temporal analysis was performed of one of the lines, chosen because there was a more synchronous engagement of apoptosis (Figure 3A and B), both 300 kbp and 50 kbp fragments were observed up to 3 h and thereafter were degraded. These sizes of fragments have been suggested to

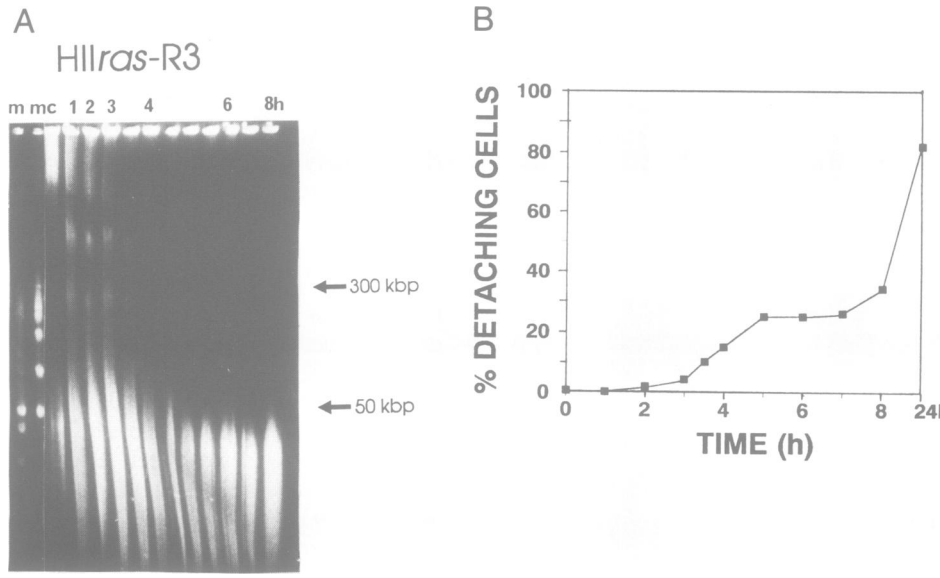

Fig. 3. (**A**) FIGE of the DNA from H11ras-R3 rat fibroblasts, from combined attached and detached cells (see Materials and methods), after the withdrawal of serum. Cells were collected hourly for the first 3 h, half-hourly up to 6 h and hourly thereafter. (**B**) The kinetics of detachment of cells from the monolayer after serum withdrawal. (c, controls of attached cells at time zero; m, molecular weight markers.)

arise from the release of loops (50 kbp) or rosettes (300 kbp) of chromatin, perhaps as they become detached from their attachment points on the nuclear scaffold (Filipski *et al.*, 1990). When apoptosis was asynchronous, such as in the HT-29-I1, CC164 and DU-145 cells, we were unable to detect 300 kbp fragments. Interestingly, in DU-145 cells, although discrete 50 kbp fragments were observed during apoptotic cell death there was neither simultaneous nor subsequent cleavage to 180–200 bp integer fragments.

The MCF-7 mammary carcinoma cells deprived of serum did not exhibit a classical apoptotic morphology (Figure 1e) nor did they exhibit discrete DNA fragmentation patterns. This is not the first report showing that mammary epithelia fail to exhibit the DNA fragmentation pattern classified as being associated with apoptosis. In recent study using end-labelling for the detection of DNA strand breaks in several tissues, including colon, ovary and thymocytes (Gavrieli *et al.*, 1992), only the involution of the murine mammary gland, after weaning, failed to show DNA breaks indicative of the early stages of classical apoptosis. There has been controversy surrounding the mode of MCF-7 cell death: Bardon *et al.* (1987) showed that anti-estrogen treatment resulted in a heterogeneous pattern of cell death of necrosis and apoptosis, and Isaacs and colleagues have also suggested heterogeneity of the mode of MCF-7 cell death (Kyprianou *et al.*, 1991).

The reasons for the resistance of DU-145 cell nuclei to fragment their DNA into discrete internucleosomal integers are unclear. This could reflect a phenotypically, inherently low level or activity of an endonuclease, or a topographical difference in chromatin structure such that it is inaccessible to a pre-existing endonuclease. This latter possibility was favored by Ucker *et al.* (1992) in a careful study of cytotoxic T lymphocyte-mediated killing of murine fibroblasts, where genome digestion was considered to be limited by the accessibility of chromatin to endonucleolytic attack. Whether or not these assumptions are correct, our results suggest first, that the appearance of a DNA 'ladder' is not mandatory in an apoptotic cell death defined by characteristic changes in chromatin condensation and secondly, that this appears to be a late event, not coincident with chromatin condensation. Interestingly, in *Caenorhabditis elegans* the activity of the *nuc-1*-encoded endonuclease is believed to function after the

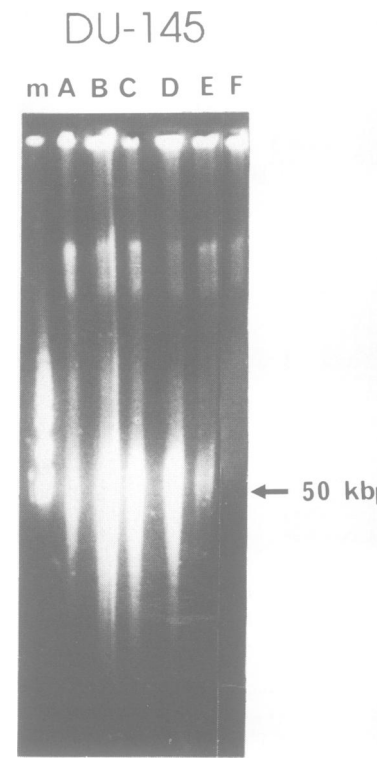

Fig. 4. FIGE of the DNA from detached DU-145 androgen-independent prostate carcinoma cells collected at every 2 h intervals between 0–10 h (**A**), 10–18 h (**B**), 20–24 h (**C**), 26–32 h (**D**) and 34–36 h (**E**) after the addition of 25 μM of the topoisomerase II poison VP16 (DU-145). (F, monolayer control at time zero; m, molecular weight markers.)

phagocytosis of cells which have undergone programmed cell death, and mutations in this locus do not inhibit programmed cell death (reviewed by Ellis and Horvitz, 1991). This supports the idea that degradation of DNA to oligonucleosome fragments is a late event and that in mammalian epithelial and mesenchymal cells (our results and Ucker *et al.*, 1992) it is either similarly late, or is absent. What are the events which initiate the earlier changes in DNA integrity, and are these events critical to the engagement of apoptosis? Proteolysis of lamin B and topoisomerases I and II has been observed during the drug-induced apoptosis of myeloid (Kaufmann, 1989) and mesenchymal cells (Ucker *et al.*, 1992) so that it is possible that events at the nuclear membrane and matrix may precede internucleosomal cleavage of DNA by an endonuclease(s). Chromatin is attached to this internal nuclear matrix and peripheral lamina to establish domains of chromatin structure. The enzyme topoisomerase II plays a critical role in this structure, both as an anchor between DNA and the protein components of the scaffold, and as a mediator of changes in DNA topology (Mirkovitch *et al.*, 1984; Adachi *et al.*, 1991; Roberge and Gasser, 1992). Topoisomerase II molecules appear to be located with a periodicity of 300 kbp along chromatin (Filipski *et al.*, 1990) and the transient appearance of 300 kbp fragments during the early stages of apoptosis stimulated by serum withdrawal in H11ras-R3 cells suggests a role for topoisomerase II in the earliest stages of apoptosis (Figure 3). Subsequent endonucleolytic activity at the sites of the anchorage of loop domains to the nuclear scaffold releases DNA fragments of 50 kbp. That identical fragmentation to 50 kbp units was induced in a number of different cell types by several disparate stressful stimuli such as serum withdrawal, a topoisomerase II inhibitor and TGF-β1, provides evidence that this is a critical step in the DNA degradation of apoptosis. This indeed suggests that the signals for apoptosis may be transduced to the nuclear scaffold prior to the activation of endonucleolytic DNA cleavage. Recent reports which implicate DNAse I activity in apoptosis (Ucker *et al.*, 1992; Pietsch *et al.*, 1993) have led to speculation that cytoskeletal changes may play a role in the initiation of DNA cleavage.

Arguments, some semantic, of what constitutes an apoptotic or a programmed cell death (Lockshin and Zachary, 1991) will continue unless key biochemical features of the process are described, particularly those which are highly conserved. Proposals which suggest that apoptosis is essentially characterized by the internucleosomal cleavage of DNA have relied upon the well-defined features of thymocyte and lymphocyte apoptosis (Compton, 1992). Ongoing attempts to identify and purify the endonuclease(s) responsible for this cleavage are driven by the idea that the signals for cell death may be transduced directly to the endonuclease. The work presented here provides evidence that earlier changes in the integrity of DNA precede internucleosomal cleavage, and the loci elsewhere might profitably be investigated as the recipients of signals for the engagement of cell death. Answers to the converse and important question of why some tumor cells are resistant to apoptotic cell death via expression of certain apoptosis-suppressing oncogenes, such as the nuclear membrane-associated *bcl*-2 (Jacobson *et al.*, 1993), will also be more readily achieved as the sequence of events culminating in the irreversible commitment to apoptosis are elucidated.

Materials and methods

Cell lines and culture conditions

DU-145 human androgen-independent prostatic cancer cells were kindly provided by Dr John S.Lazo, Department of Pharmacology, Pittsburg University Medical School, PA. They were maintained in RPMI 1640 medium supplemented with 10% fetal calf serum (FCS), glutamine and antibiotics. Cells were routinely seeded on day 0 at 5×10^5 cells per 75 cm^3 flask and treated with VP-16 at 25 μM on day 5. The resulting detached cells were collected every 2 h over the subsequent 2 days. MCF-7 human mammary carcinoma cells were kindly provided by Dr W.Bursch (Institute of Tumor Biology, Vienna) and were maintained in DMEM medium supplemented with 10% FCS, glutamine and antibiotics. Cultures were routinely divided at a ratio of 1:10 or 1:20 and fed until confluence. Serum was then reduced to 0.25%. Cells started to detach 24–36 h after the reduction of serum and were collected at the intervals indicated. H11ras-R3 (RE423) cells were revertants of HPV11 and *ras*-transformed rat fibroblasts, kindly provided by Dr C.Cerni (Institute of Tumor Biology, Vienna), and were maintained in DMEM medium supplemented with 10% FCS, glutamine and gentamycin. Monolayers were divided 1:5 and fed every 4 days. Two days after reaching confluence, the serum was reduced to 0.25% whereupon the cells underwent rapid detachment (within 3–4 h). The kinetics of detachment and the morphology of detached cells were assessed. At each time point, both the detached and attached cells were combined and $\sim 10^5$ cells were reserved for FIGE such that the proportion of detached cells in the combined sample increased with time. This cellular system will be described in detail elsewhere. A clone of the Mv1Lu mink lung epithelial cell line (designated CC164, American Type Culture Collection), which is sensitive to TGF-β1, was kindly provided by Dr M.Vetterlein (Institute of Histology–Embryology, University of Innsbruck, Austria). Cells were cultured in DMEM supplemented with 10% FCS, glutamine and antibiotics. Confluent cultures were divided 1:20 and grown until they reached 50–70% confluence prior to reduction of FCS to 0.25%. After 36 h, cells were stimulated to die by the addition of 10% FCS and 10 ng/ml of recombinant TGF-β1, kindly provided by Dr Clare Heyworth (Paterson Institute, Manchester). Asynchronous cell death began 24–72 h later and the detached cells were collected from 24 h onwards, at the intervals indicated. HT-29-I1 human colon adenocarcinoma cells were provided by Dr E.A.Friedman (Memorial Sloane-Kettering Center, New York) and grown in DMEM medium supplemented with 10% FCS, glutamine and antibiotics. Cells were divided at a ratio of 1:10 and fed every 3–4 days until confluence, when they began to detach from the monolayer. These were collected at the times shown. All cell lines were maintained in an atmosphere of 5% CO_2/95% air at 37°C.

Morphological examination of cells

Detached cells were counted by hemocytometer and resuspended in phosphate buffered normal saline at $\sim 10^7$ cells/ml. 100 μl of cell suspension was fixed with 100 μl of 3% paraformaldehyde and smears of 10 μl aliquots laid on glass slides coated with 3-aminopropyl-triethoxysilane. For inspection of chromatin, cells were stained with 8 μg/ml of Hoeschst 33258 and mounted in Mowiol. Microscopy was performed under conditions of normal illumination and fluorescent light, using phase contrast optics.

Sample preparation

In all cases, except the H11ras-R3 cells described above, cells which detached from the monolayers following serum deprivation or treatment with various agents, were harvested intermittently (generally every 2 h), pelleted by centrifugation at 1500 *g* for 5 min at 4°C and stored at −70°C. Pellets were subsequently combined such that they contained 2×10^6 cells ($\sim 10-20$ μg of DNA). Cell pellets were prepared for electrophoresis by one of two methods (Kokileva, 1989). Either they were lysed directly in 1% SDS (50 μl), then samples were loaded directly into wells on a 1.5% agarose gel; these were then capped with 50 μl of 1% low melting point agarose before being subjected to FIGE. Alternatively, cell pellets were resuspended in 25 μl of L-buffer [0.01 M Tris–Cl, 0.1 M EDTA (pH 7.6), 0.02 M NaCl], at 37°C and 25 μl of prewarmed low melting point agarose (1% in L-buffer) was added with gentle mixing. Plugs were formed on ice for 10 min and then transferred into 1 ml 1% sarcosylate (in L-buffer) supplemented with 0.1 mg/ml proteinase K and incubated overnight at 37°C. Both the plug and the supernatant were used for electrophoresis. Plugs were either used directly or were stored in 500 mM EDTA at 4°C. Low molecular weight DNA that had leached out of the plugs during incubation was precipitated over 48 h by adding 0.2 vol of 10.5 M ammonium acetate and 2 vol of absolute ethanol. This DNA was then analyzed by conventional gel electrophoresis.

Field inversion gel electrophoresis

FIGE was carried out according to the method of Filipski *et al.* (1990). Briefly, electrophoresis was carried out using a horizontal gel chamber, a model 200/20 power supply and Pulsewave 760 switcher (Bio-Rad Laboratories). The gels were run at 150 V in 10 mM Tris–acetate, pH 8.6 and 1 mM EDTA with a ramping rate changing from T_1 = 0.5 s to T_2 = 10 s for the first 19 h and from T'_1 = 10 s to T'_2 = 60 s for the next 19 h, with a forward to backward ratio of 3 at 4°C using 1.5% electrophoresis grade agarose (Flowgen). After electrophoresis, the gel was stained with ethidium bromide (0.5 μg/ml; 45 min) and then destained in water (1 h). Gels were incubated with RNase A (Sigma) (0.5 mg/ml in running buffer) for 2–3 h, at 37°C, after destaining. The gel was viewed using a UV transilluminator and photographed using Polaroid 667 film. Molecular weight markers ('Pulse Marker', 50–1000 kbp) were purchased from Sigma.

Conventional agarose gel electrophoresis

Cell pellets, of equivalent cell number, were prepared in parallel to those used for FIGE, lysed in 1% SDS, loaded directly into wells on a 1.5% agarose gel and the wells capped with agarose. Electrophoresis was carried out at 50 V (constant) for 3 h at room temperature using 40 mM Tris–acetate/4 mM EDTA running buffer. After electrophoresis, the gel was stained with ethidium bromide (0.5 μg/ml; 15 min) and then destained in water (30 min). Gels were incubated with RNase A (0.5 mg/ml in running buffer) for 1–2 h at 37°C after destaining. The gel was viewed using a UV transilluminator and photographed using Polaroid 667 film.

Acknowledgements

We thank Dr B.Kamera (Institute of Tumor Biology, Vienna) for data on the sensitivity of CC1-64 cells to TGF-β1 and Dr Ged Brady for criticism of the manuscript. We are grateful to the European Science Foundation for the award of an Exchange Fellowship in Toxicology to Franziska Oberhammer. This work was supported by grants from the Cancer Research Campaign and Zeneca Pharmaceuticals.

References

Adachi,Y., Luke,M. and Laemmli,U.K. (1991) *Cell*, **64**, 137–148.
Arends,M.J., Morris,R.G. and Wyllie,A.H. (1990) *Am. J. Pathol.*, **136**, 593–608.
Bardon,S., Vignon,F., Montcourrier,P. and Rochefort,H. (1987) *Cancer Res.*, **47**, 1441–1448.
Barres,B.A., Hart,I.K., Coles,H.S.R., Burne,J.F., Voyvodic,J.T., Richardson,W.D. and Raff,M.C. (1992) *Cell*, **70**, 31–46.
Barry,M.A. and Eastman,A. (1993) *Arch. Biochem. Biophys.*, **300**, 440–450.
Brown,D.G., Sun,X.-M. and Cohen,G.M. (1993) *J. Biol. Chem.*, **268**, 3037–3039.
Carle,G.F., Frank,M. and Olson,M.V. (1986) *Science*, **232**, 65–68.
Caron-Leslie,L.M., Schwartzman,R.A., Gaido,M.L., Compton,M.M. and Cidlowski,J.A. (1991) *J. Steroid Biochem.*, **40**, 661–671.
Cohen,G.M., Sun,X.-M., Snowden,R.T., Dinsdale,D. and Skilleter,D.N. (1992) *Biochem. J.*, **286**, 331–334.
Compton,M.M. (1992) *Cancer Metastasis Rev.*, **11**, 105–119.
Dive,C. and Wyllie,A.H. (1993) In Hickman,J.A. and Tritton,T.R. (eds), *Frontiers in Pharmacology: Cancer Chemotherapy*. Blackwell, Oxford, pp. 21–56.
Ellis,R.E. and Horvitz,H.R. (1991) *Development*, **112**, 591–603.
Filipski,J., Leblanc,J., Youdale,T., Sikorska,M. and Walker,P.R. (1990) *EMBO J.*, **9**, 1319–1327.
Gavrieli,Y., Sherman,Y. and Ben-Sasson,A. (1992) *J. Cell Biol.*, **119**, 493–501.
Hickman,J.A. (1992) *Cancer Metastasis Rev.*, **11**, 121–139.
Jacobson,M.D., Burne,J.F., King,M.P., Miyashita,T., Reed,J.C. and Raff,M.C. (1993) *Nature*, **361**, 365–369.
Kaufmann,S.H. (1989) *Cancer Res.*, **49**, 5870–5878.
Kokileva,L. (1989) *Mol. Biol. Reports*, **13**, 139–143.
Kyprianou,N., English,H.F., Davidson,N.E. and Issacs,J.T. (1991) *Cancer Res.*, **51**, 162–166.
Lockshin,R.A. and Zachary,Z. (1991) In Tomei,L.D. and Cope,F.O. (eds), *Apoptosis: The Molecular Basis of Cell Death*. Cold Spring Harbor Laboratory Press, Cold Spring Harbor, NY, pp. 47–60.
Mirkovitch,J., Mirault,M.-E. and Laemmli,Y.K. (1984) *Cell*, **39**, 223–232.
Oberhammer,F., Fritsch,G., Schmied,M., Pavelka,M., Printz,D., Purchio,T., Lassman,H. and Schulte-Hermann,R. (1993) *J. Cell Sci.*, **104**, 317–326.
Peitsch,M.C., Polzar,B., Stephan,H., Crompton,T., MacDonald,H.R., Mannherz,H.G. and Tschopp,J. (1993) *EMBO J.*, **12**, 371–377.
Roberge,M. and Gasser,S.M. (1992) *Mol. Microbiol.*, **6**, 419–423.
Roy,C., Brown,D.L., Little,J.E., Valentine,B.K., Walker,P.R., Sikorska,M., Leblanc,J. and Chaly,N. (1992) *Exp. Cell Res.*, **200**, 416–424.
Tomei,L.D., Shapiro,J.P. and Cope,F.O. (1993) *Proc. Natl Acad. Sci. USA*, **90**, 853–857.
Ucker,D.S., Obermiller,P.S., Eckhart,W., Apgar,J.R., Berger,N.A. and Meyers,J. (1992) *Mol. Cell. Biol.*, **12**, 3060–3069.
Walker,P.R., Smith,C., Youdale,T., Leblanc,J., Whifield,J.F. and Sikorska,M. (1991) *Cancer Res.*, **51**, 1078–1085.
Wyllie,A.H. (1980) *Nature*, **284**, 555–556.
Wyllie,A.H. (1992) *Cancer Metastasis Rev.*, **11**, 95–103.

Received on March 18, 1993; revised on May 10, 1993